Rabbit hindlimb kinematics and ground contact kinetics during the stance phase of gait

Patrick Hall [1], Caleb Stubbs [1], David E Anderson [2], Cheryl Greenacre [3], Dustin L Crouch [Corresp. 1]

[1] Mechanical, Aerospace, and Biomedical Engineering, University of Tennessee - Knoxville, Knoxville, Tennessee, United States

[2] Department of Large Animal Sciences, University of Tennessee - Knoxville, Knoxville, Tennessee, United States

[3] Department of Small Animal Sciences, University of Tennessee - Knoxville, Knoxville, Tennessee, United States

Corresponding Author: Dustin L Crouch
Email address: dcrouch3@utk.edu

Though the rabbit is a common animal model in musculoskeletal research, there are very limited data reported on healthy rabbit biomechanics. Our objective was to quantify the normative hindlimb biomechanics (kinematics and kinetics) of six New Zealand White rabbits (3 male, 3 female) during the stance phase of gait. We measured biomechanics by synchronously recording sagittal plane motion and ground contact pressure using a video camera and pressure-sensitive mat, respectively. Both foot angle (i.e., angle between foot and ground) and ankle angle curves were unimodal. The maximum ankle dorsiflexion angle was 66.4 ± 13.4° (mean ± standard deviation across rabbits) and occurred at 38% stance, while the maximum ankle plantarflexion angle was 137.2 ± 4.8° at toe-off. Minimum and maximum foot angles were 17.2°±6.3° at 10% stance and 123.3°±3.6° at toe-off, respectively. The maximum peak plantar pressure and plantar contact area were

21.7 ± 4.6 %BW/cm^2 and 7.4 ± 0.8 cm^2 respectively. The maximum net vertical ground reaction force and vertical impulse, averaged across rabbits, were 44.0 ± 10.6 %BW and 10.9 ± 3.7 %BW•s, respectively. Stance duration (0.40 ± 0.15 s) was statistically significantly correlated (p<0.05) with vertical impulse (Spearman's ρ = 0.76), minimum foot angle (ρ = -0.58), plantar contact length (ρ = 0.52), maximum foot angle (ρ = 0.41), and minimum foot angle (ρ = -0.30). Our study confirmed that rabbits exhibit a digitigrade gait pattern during locomotion. Future studies can reference our data to quantify the extent to which clinical interventions affect rabbit biomechanics.

4   Rabbit Hindlimb Kinematics and Ground Contact Kinetics During the Stance Phase of Gait

6   Authors: Patrick T. Hall[1], Caleb Stubbs[1], David E. Anderson[2], Cheryl Greenacre[3], Dustin L.
7   Crouch[1]

9   [1]University of Tennessee, Knoxville – Department of Mechanical, Aerospace, and Biomedical
10   Engineering
11   [2]University of Tennessee, Knoxville – Department of Large Animal Sciences
12   [3]University of Tennessee, Knoxville – Department of Small Animal Sciences

14   Corresponding author contact:
15   Phone: (919) 670-4234
16   Email: dcrouch3@utk.edu

17   Keywords: Rabbit, Biomechanics, Noninvasive, Stance
18   Word Count: 3265

Abstract

Though the rabbit is a common animal model in musculoskeletal research, there are very limited data reported on healthy rabbit biomechanics. Our objective was to quantify the normative hindlimb biomechanics (kinematics and kinetics) of six New Zealand White rabbits (3 male, 3 female) during the stance phase of gait. We measured biomechanics by synchronously recording sagittal plane motion and ground contact pressure using a video camera and pressure-sensitive mat, respectively. Both foot angle (i.e., angle between foot and ground) and ankle angle curves were unimodal. The maximum ankle dorsiflexion angle was 66.4 ± 13.4° (mean ± standard deviation across rabbits) and occurred at 38% stance, while the maximum ankle plantarflexion angle was 137.2 ± 4.8° at toe-off. Minimum and maximum foot angles were 17.2°±6.3° at 10% stance and 123.3°±3.6° at toe-off, respectively. The maximum peak plantar pressure and plantar contact area were 21.7 ± 4.6 %BW/cm^2 and 7.4 ± 0.8 cm^2 respectively. The maximum net vertical ground reaction force and vertical impulse, averaged across rabbits, were 44.0 ± 10.6 %BW and 10.9 ± 3.7 %BW·s, respectively. Stance duration (0.40 ± 0.15 s) was statistically significantly correlated ($p<0.05$) with vertical impulse (Spearman's ρ = 0.76), minimum foot angle (ρ = -0.58), plantar contact length (ρ = 0.52), maximum foot angle (ρ = 0.41), and minimum foot angle (ρ = -0.30). Our study confirmed that rabbits exhibit a digitigrade gait pattern during locomotion. Future studies can reference our data to quantify the extent to which clinical interventions affect rabbit biomechanics.

Introduction

48

49   The rabbit is a common animal model in musculoskeletal research to, for example, test

50 new potential clinical interventions or study the response of tissues to mechanical stimuli. Some

51 interventions would be expected to affect the motor function of the hindlimb ankle and foot.

52 Examples of such interventions include tenotomy of ankle dorsiflexor (Abrams et al. 2000) or

53 plantarflexor (Nagasawa et al. 2008; Reddy et al. 1998) muscles, immobilization of the knee

54 and/or ankle joint (Gossman et al. 1986; Ponten & Friden 2008; Sjostrom et al. 1979), and

55 release of tendon retinacula to manipulate muscle-tendon moment arms (Koh & Herzog 1998b;

56 Reddy & Gupta 2007). Recently, we adopted a rabbit model to test the feasibility of a new type

57 of ankle-foot prosthesis (Hall et al. 2021). For potential clinical interventions, quantifying their

58 effect on motor function will be valuable, if not essential, for achieving clinical translation.

59   One way to quantify motor function is by measuring biomechanical variables. The effect

60 of an intervention could be determined by comparing biomechanical data between animals that

61 did and did not receive the intervention. Unfortunately, the hindlimb biomechanics of healthy

62 rabbits has not been well characterized. We are aware of only one previous study in which

63 multi-sample data were limited to knee and ankle kinetics (i.e., joint moments) during gait

64 (Gushue et al. 2005). A more comprehensive dataset on normative rabbit hindlimb

65 biomechanics in the literature would (1) make it easier for researchers to determine the effects

66 of experimental interventions on motor function, (2) reduce the number of healthy animals used

67 as experimental controls, and (3) increase basic understanding about animal locomotion.

68   Two common, broad measures of hindlimb biomechanics that have not been reported

69 for a multi-sample rabbit cohort are joint kinematics and ground contact kinetics. For example,

70 rabbits are considered to have a "plantigrade type" foot morphology (Kimura 1996) but a

71 digitigrade gait pattern during locomotion (Blair 2013; Volait-Rosset et al. 2019). Unfortunately,

72 there are no published kinematic data to quantitatively verify such statements about the

73 hindlimb gait patterns of rabbits. In terms of ground contact kinetics, one previous study

74 reported that the net vertical ground reaction force curve during hindlimb stance phase

75 displayed a slight bimodal pattern with a maximum force of nearly 60% body weight (Gushue et

76 al. 2005); However, these kinetic data were presented for only one rabbit and one trial;

77 therefore, it is unclear if the patterns and values are consistent across multiple rabbits and trials.

78   The goal of our study was to quantify hindlimb ankle and foot kinematics and ground

79 contact kinetics during the stance phase of gait in healthy rabbits (i.e., rabbits that have not

80 received an experimental intervention). Summary results are presented below, and the raw data

81 are available online as supplementary data. The new biomechanics data will serve as a

82 valuable reference for interventional studies involving rabbits and improve our basic

83 understanding about rabbit locomotion.

84 Materials & Methods

85   All animal procedures were approved by the University of Tennessee, Knoxville

86 Institutional Animal Care and Use Committee (protocol #2637). We used a cross-sectional study

87 design, measuring biomechanics in one test session from both hindlimbs of six (3 male, 3

88 female) healthy, standard laboratory New Zealand White (NZW) rabbits (Charles River

89 Laboratories, Wilmington, MA). The rabbits represented a convenience sample as they were

90 part of another larger, iterative, non-hypothesis-driven study to test a novel orthopedic implant

91 (Hall et al. 2021); thus, no power analysis was performed for either study. Since this was not a

92 clinical trial, there were no separate experimental groups. At the time of testing, the rabbits were

93 16 weeks old and weighed 2.7 ± 0.33 kg. Each rabbit was considered one experimental unit.

94 Rabbits were housed individually in adjacent crates, fed *ad libitum* with a standard laboratory

95 diet and Timothy hay, and given daily enrichment and positive human interaction.

96   The setup for our locomotor measurement system included several components (Fig. 1).

97   A 4-tile pressure mat (Very High Resolution Walkway 4, Tekscan, Inc., South Boston, MA) was

98   used to record pressure data at 60 Hz. We taped 320-grit sandpaper to the top of the smooth

99   pressure-sensing area to prevent the rabbits from slipping. Each tile was calibrated

100   independently using a 3-kg mass with three separate felt pads that each approximated the

101   geometry and texture of the rabbit hindlimb plantar surface. The mat was placed inside a clear

102   acrylic tunnel, which constrained the rabbits to ambulate along the mat. The mat width (11.2 cm)

103   permitted only unilateral pressure measurements; therefore, to record data for both hindlimbs,

104   we laterally offset the mat in the tunnel and had the rabbit ambulate through the tunnel in both

105   directions, as described below. A camera (1080P HD Webcam, SVPRO), placed three feet

106   away from the clear acrylic panel, captured video at 60 Hz. Video and pressure mat data were

107   synchronized using the Tekscan Walkway software (Tekscan, South Boston, MA).

108   During a two-week acclimation period prior to testing, rabbits were trained to ambulate

109   through the acrylic tunnel when given negative reinforcement (i.e., prodding). Then, at the

110   beginning of the test session, we shaved both hindlimbs and marked the metatarsophalangeal

111   (MTP), ankle, and knee joint centers on the lateral side of each hindlimb with black ink (Fig. 2A)

112   to facilitate calculation of joint kinematics from the videos. After marking, we placed the rabbit

113   into a pen with the acrylic tunnel and pressure mat. Each trial began when the rabbit entered the

114   tunnel. A trial was deemed successful if (1) the rabbit continued moving through the entire

115   length of the tunnel without stopping, (2) all hindlimb markers were visible in the video frame

116   during a stance phase, and (3) the entire plantar contact area was within the sensing area of the

117   pressure mat. These criteria were checked both during and after the test session. The session

118   continued until we collected data for 5-7 successful trials of gait through the tunnel in each

119   direction. The direction of gait is a potential confounder, which we address as a limitation in the

120   Discussion section.

121   All confirmed successful trials – 6 to 10 trials per rabbit, 49 trials in all - were selected for

122   analysis. We calculated joint angles from the video frames corresponding to stance phase using

123   a custom script in MATLAB (Mathworks, Natick, MA). The program used a bottom-hat

124   morphology filter (*imbothat* function in MATLAB) to distinguish the black ink marks and calculate

125   the centroid of each marker position (Fig. 2B). Then, frame-by-frame, we visually verified the

126   marker centroids and, if the centroid location appeared inaccurate, corrected the location by

127   manually approximating the centroid from the still frame. Calculating marker positions from a

128   two-dimensional video frame assumes that all markers lie in a plane that is parallel to the video

129   frame; this was a reasonable assumption given the arrangement of the camera with respect to

130   the acrylic tunnel. Finally, we calculated the angle between the foot segment and ground (i.e.,

131   foot angle) and between the foot and shank segments (i.e., ankle angle) throughout stance (Fig.

132   2C). Since the camera was approximately level with the ground, we defined the ground as a

133   horizontal line in the video frame. Ankle angles >90° and <90° corresponded to plantarflexion

134   and dorsiflexion, respectively.

135   Ground contact pressure data were processed using the Tekscan Walkway software.

136   Each hind foot was isolated by drawing a strike box around the corresponding pressure map.

137   From the pressure map in the strike box and for each time point, we computed (1) peak and

138   average plantar pressures, (2) plantar contact area and length, (3) net vertical ground reaction

139   force (vGRF), and (4) vertical impulse. The contact area was calculated at each timepoint as the

140   total geometric area within the strike box for which the pressure was greater than zero. The

141   plantar contact length was the total cranial-caudal length of the plantar surface that contacted

142   the ground at any time during stance; plantar contact length was expressed as a percentage of

143   the total length of the plantar surface, measured from unsuccessful trials during which the rabbit

144   stopped and placed the entire plantar surface on the pressure mat. The vGRF was calculated

145   as the product of foot contact area and the average pressure across the contact area. Vertical

146   impulse was calculated as the time integral of the vGRF curve. Pressure, vGRF, and vertical

147   impulse values were normalized by body weight.

148   We computed the stance duration for each limb as the length of time for which pressure

149   was greater than zero within the limb's strike box. The timepoints of time-series biomechanical

150   data were normalized by the stance duration; at each normalized timepoint, data were averaged

151   across trials for each rabbit, then averaged across rabbits. Similarly, plantar contact length and

152   vertical impulse were averaged across trials for each rabbit, then averaged across rabbits.

153   We observed that stance duration across trials (n = 49) had a relatively high variation

154   and exhibited a right-skewed distribution (mean = 0.40 s, median = 0.35 s, standard deviation =

155   0.15 s). Since gait biomechanics are known to vary with gait speed during bipedal (Lelas et al.

156   2003) and quadrupedal (Boakye et al. 2020) locomotion, we tested whether stance duration was

157   significantly correlated with select biomechanical outcome variables (Table 1). Given that stance

158   duration was not normally distributed, we used the non-parametric Spearman's rank-order

159   correlation test. We computed Spearman's correlation coefficient (ρ) to determine the strength

160   and direction of correlation. Strength was interpreted based on the magnitude of ρ as previously

161   reported (Chan 2003). The correlation was considered statistically significant for $p<0.05$. For the

162   correlation test, we considered each trial as an independent sample.

163   ## Results

164   At foot strike, the ankle angle became increasingly dorsiflexed for the first 38% of

165   stance, then increasingly plantarflexed for the remaining 62% of stance (Fig. 3A); these phases

166   are sometimes referred to as "loading response" and "forward propulsion", respectively (Li &

167   Hsiao-Wecksler 2013). The maximum ankle dorsiflexion angle during stance was 66.4 ± 13.4°

168   (mean ± standard deviation). The ankle was plantarflexed (>90°) at both foot strike (103.1 ±

169   13.0°) and toe-off (137.2 ± 4.8°), with the maximum ankle plantarflexion angle during stance

170 occurring at toe-off. The foot maintained a positive angle throughout stance, starting at 21.1 ±

171 6.9°, then decreasing to a minimum foot ankle of 17.2 ± 6.3° at 10% stance (Fig. 3B).

172 Thereafter, the foot ankle gradually increased up to 123.3 ± 3.6° at toe-off, indicating that the

173 foot had rotated beyond a vertical orientation (90°).

174   Peak plantar pressure over the stance phase was unimodal, reaching a maximum of

175 21.7 ± 4.6 %BW/cm^2 at 33% stance (Fig. 4A). By comparison, average plantar pressure over

176 the entire plantar contact area was nearly uniform between 5% and 95% stance, with the mean

177 ranging from 4.3 – 6.4 %BW/cm^2 over that interval (Fig. 4B). The maximum peak plantar

178 pressure (21.7 %BW/cm^2) was over 3x larger than the maximum average plantar pressure (6.4

179 %BW/cm^2). The vGRF curve over stance was unimodal, with a maximum of 44.0 ± 10.6 %BW

180 that occurred at 27% stance (Fig. 5). Vertical impulse was 10.9 ± 3.7 %BW·s.

181   The plantar contact area curve was unimodal (Fig. 6); the maximum plantar contact area

182 was 7.4 ± 0.8 cm^2 and occurred at 21% stance. The plantar contact length was, on average, 70

183 ± 11% of the total plantar surface length and ranged from 41-95% across all trials. The plantar

184 contact length was shifted entirely toward the cranial aspect of the plantar surface (i.e., toes),

185 indicating that the rabbits exhibited a digitigrade gait pattern.

186   Stance duration was significantly correlated with several biomechanical outcome

187 variables (Table 1). There was a strong, positive correlation between stance duration and

188 vertical impulse (ρ = 0.76, p < 0.001). Stance duration had fair-to-moderate correlation with

189 minimum foot angle (ρ = -0.58, p < 0.001) and plantar contact length (ρ = 0.52, p < 0.001).

190 Maximum foot angle (ρ = 0.41, p = 0.003), minimum ankle angle (ρ = -0.30, p = 0.034), and

191 maximum vGRF (ρ = -0.35, p = 0.014) had fair correlation with stance duration.

Discussion

192

193   Rabbits are among the few mammals that almost exclusively exhibit a bounding or half-

194 bounding gait in which the hindlimbs push off and move together (Dagg 1973). Other mammals,

195 such as rats, mice, cats, and squirrels, use a bounding gait at fast gait speeds but a different

196 gait pattern (e.g., walking) at slow gait speeds. To our knowledge, there are few sources that

197 present biomechanical data for rabbits that are similar to our data; thus, below, we primarily

198 discuss our results in the context of those reported for other quadrupedal species. Though we

199 did not directly measure gait speed, the stance duration of 0.40 ± 0.15 s for our rabbits is

200 consistent with a walking gait speed (about 0.6 m/s) in cats (Goslow Jr. et al. 1973; Verdugo et

201 al. 2013).

202   vGRF data have been reported for only one rabbit (Gushue et al. 2005) and,

203 unsurprisingly, are not representative of the average vGRF values we observed across multiple

204 rabbits and trials. For example, the reported vGRF was bimodal and had a maximum of greater

205 than 50 %BW (Gushue et al. 2005); by comparison, the average vGRF curve in our study was

206 unimodal and had a maximum of 44 %BW. This maximum vGRF was similar to that of cats

207 (Verdugo et al. 2013) and dogs (Besancon et al. 2003) during walking. Conversely, vertical

208 impulse was lower in the rabbits (~11 %BW·s) than in cats (~13 %BW·s) (Verdugo et al. 2013)

209 and dogs (~18 %BW·s) (Besancon et al. 2003) during walking.

210   Compared to maximum ground contact kinetic data, time-series kinetic data have not

211 been widely reported in animals. Studies have reported time-series pressures under different

212 plantar regions in, for example, dogs (Marghitu et al. 2003) and bonobos (Vereecke et al. 2003).

213 The time-series pressure curves in dogs were unimodal (Marghitu et al. 2003), similar to our

214 rabbits. Time-series ground contact kinetics should be reported more frequently, at least as

215 supplementary data, as they provide more detailed information than maximum values.

216   The plantar contact length data confirmed that rabbits exhibit a digitigrade gait pattern,

217   consistent with previous qualitative descriptions of rabbit gait (Blair 2013; Volait-Rosset et al.

218   2019). Most mammals use a digitigrade gait pattern during locomotion, which is more efficient

219   than the plantigrade gait of humans (Cunningham et al. 2010). The rabbits' foot and ankle

220   kinematics were generally similar to those of rats during walking (Bauman & Chang 2010;

221   Varejao et al. 2002). Specifically, in both rabbits and rats, the ankle joint angle curve during

222   stance was nearly unimodal. The ankle progressed from an initial, slightly plantarflexed posture

223   to a dorsiflexed posture that peaked around mid-stance, then returned to a plantarflexed posture

224   at terminal stance (Bauman & Chang 2010; Varejao et al. 2002). Foot angle is not commonly

225   reported but, qualitatively, rats progressed from a low to high foot angle during stance similar to

226   the rabbits in our study (Varejao et al. 2002).

227   Based on the correlation coefficients (Table 1), there were several statistically significant

228   relationships between stance duration and other biomechanical outcome variables. Specifically,

229   for shorter stance durations, the hindlimb exhibited (1) shorter plantar contact lengths (i.e., more

230   extreme digitigrade gait), (2) a more-vertical foot posture, (3) lesser maximum ankle

231   dorsiflexion, (4) greater maximum vertical force (vGRF), and (5) lesser vertical impulse. In both

232   quadrupeds (Goslow Jr. et al. 1973; Vilensky 1987) and humans (Fukuchi et al. 2019), stance

233   duration decreases as gait speed increases. Assuming that the same was true for the rabbits in

234   our study (though we did not measure gait speed directly), our correlations were generally

235   consistent with those reported previously. For example, the ankle is also less dorsiflexed (i.e.,

236   more plantarflexed) at faster walking speeds (i.e., shorter stance durations) in humans (Fukuchi

237   et al. 2019), cats (Goslow Jr. et al. 1973), and pigs (Mirkiani et al. 2022). Cats also have greater

238   maximum vertical forces and lesser vertical impulse at faster walking speeds (i.e., shorter

239   stance durations) (Liu et al. 2020).

240   We chose an approach to measure rabbit hindlimb biomechanics that is practical for

241   longitudinal interventional studies in rabbits. For example, we used a video-based motion

242   capture method to quantify hindlimb kinematics from ink-based skin markers. Conversely, state-

243   of-the-art methods track flat or spherical reflective markers that are placed on the skin using

244   adhesive tape. Ink-based markers stay on the skin more reliably than adhesive markers that can

245   fall off during test sessions. However, any markers placed on the skin are prone to skin motion

246   artifact and inaccurate marker placement relative to the joint center. In our study, skin motion

247   and marker placement error contributed to high variation (maximum-minimum) in the lengths of

248   foot (20%) and shank (40%) segments computed from marker locations in each trial. This

249   variation is consistent with the large errors in joint angles computed from skin markers in rats

250   (Bauman & Chang 2010). These errors motivate the use of more reliable motion capture

251   methods, such as reflective markers attached to transdermal bone pins (Gushue et al. 2005) or

252   radiography (Bauman & Chang 2010). Though reliable, these methods have practical

253   limitations. For example, bone pins are relatively difficult to implement, especially for longitudinal

254   studies, and may interfere with movement either mechanically or by causing discomfort. Bi-

255   plane fluoroscopy can acquire detailed kinematic data (Koh & Herzog 1998a; Tinga et al. 2018)

256   but poses a radiation safety risk to the animals and researchers. Finally, both infrared- and

257   fluoroscopy-based methods require relatively expensive equipment that must remain stationary

258   during testing and, thus, are not as accessible, portable, or mobile as video-based methods.

259   Pressure mats are, in some ways, more convenient to use with quadrupedal animals

260   than force plates, a common alternative. This is because force plates measure the resultant

261   force, which requires that only one limb contacts the plate at a time to distinguish forces among

262   limbs (Gushue et al. 2005; Jarrell et al. 2018). Conversely, pressure mats can distinguish

263   among individual limbs even if multiple limbs contact the mat simultaneously (Sheldon et al.

264   2019; Steiner et al. 2019). Considering also that force plates are generally smaller than

265   pressure mats, more gait trials may be needed to collect desired ground contact kinetic data

266   with force plates than with pressure mats. However, force plates have notable advantages. For

267   example, force plates measure forces along 6 degrees of freedom and, thus, capture all the

268   directional components of the ground-contact force, such as propulsive forces that occur in the

269   horizontal direction; conversely, pressure mats can only measure the vertical force component.

270   While both pressure mats and force plates provide reliable estimates of variables related to

271   bilateral symmetry and duration, force plates measure absolute force variables, such as

272   maximum vGRF and vertical impulse, more accurately (Oosterlinck et al. 2010).

273   Our study was limited in several ways. First, because our pressure mat was relatively

274   narrow (11.2 cm), we only measured kinematic and pressure data for one hindlimb at a time. In

275   future studies we plan to use a wider pressure mat and two cameras (one on each side) to

276   capture biomechanics data from both hindlimbs simultaneously; this data will allow us to

277   quantify temporal relationships between sides. Second, the sample frequency (60 Hz) of our

278   motion capture setup allowed us to capture stance phase only; in future studies we will use

279   cameras with a higher sample frequency to also capture the high-frequency kinematics of the

280   swing phase. Third, we computed kinematics in the sagittal plane from a single video; this had

281   practical advantages compared to multi-camera systems, as described above, but cannot reveal

282   potential effects of interventions on out-of-plane motion. Fourth, we used a custom MATLAB

283   script to compute kinematics from videos of rabbits with ink-based markers, though more

284   advanced machine-learning-based open-source software, such as DeepLabCut (Mathis et al.

285   2018a; Mathis et al. 2018b), are available. Finally, in our correlation analysis, we used stance

286   duration as a surrogate for gait speed; future studies should measure and use gait speed

287   directly since it is more customary in such analyses (Boakye et al. 2020; Lelas et al. 2003).

288   **Conclusions**

289   In conclusion, we have reported new biomechanical data based on hindlimb kinematics

290   and ground contact kinetics from healthy New Zealand White rabbits. Our results showed that

291   rabbits exhibit a digitigrade gait pattern as described in previous literature. Several

292   biomechanical values and their correlation to stance duration were similar to those observed for

293   other small mammals, such as rats, cats, and dogs. Our results add substantially to the limited

294   existing data on rabbit hindlimb biomechanics. The data can be used as an experimental control

295   to quantify the effect experimental interventions while reducing the number of animals used for

296   research. Importantly, the data can inform pre-clinical trials of musculoskeletal and other clinical

297   interventions, commonly tested in rabbits, to improve functional outcomes for human and animal

298   patients.

299 Conflict of Interest Statement

300   The authors have no conflicts of interest to report.

301 Acknowledgments

302   The authors thank Dr. Bryce Burton, Dr. Kelsey Finnie, Dr. Lori Cole, and Chris Carter

303   for veterinary care provided for the rabbits in this study, and the Office of Laboratory Animal

304   Care and Animal Housing Facility staff at the University of Tennessee, Knoxville for animal care

305   assistance. Thanks to Dr. Katrina Easton for providing constructive feedback on the manuscript.

306

307 References

308   Abrams RA, Tsai AM, Watson B, Jamali A, and Lieber RL. 2000. Skeletal muscle recovery after tenotomy
309   and 7-day delayed muscle length restoration. *Muscle & Nerve* 23:707-714.
310   Bauman JM, and Chang Y-H. 2010. High-speed X-ray video demonstrates significant skin movement
311   errors with standard optical kinematics during rat locomotion. *Journal of Neuroscience Methods*
312   186:18-24. https://doi.org/10.1016/j.jneumeth.2009.10.017

313 Besancon MF, Conzemius MG, Derrick TR, and Ritter MJ. 2003. Comparison of vertical forces in normal
314   greyhounds between force platform and pressure walkway measurement systems. *Veterinary*
315   *and Comparative Orthopaedics and Traumatology* 16:153-157.
316 Blair J. 2013. Bumblefoot: A Comparison of Clinical Presentation and Treatment of Pododermatitis in
317   Rabbits, Rodents, and Birds. *Veterinary Clinics: Exotic Animal Practice* 16:715-735.
318   10.1016/j.cvex.2013.05.002
319 Boakye M, Morehouse J, Ethridge J, Burke DA, Khattar NK, Kumar C, Manouchehri N, Streijger F, Reed R,
320   Magnuson DSK, Sherwood L, Kwon BK, and Howland DR. 2020. Treadmill-Based Gait Kinematics
321   in the Yucatan Mini Pig. *Journal of Neurotrauma* 37:2277-2291. 10.1089/neu.2020.7050
322 Chan YH. 2003. Biostatistics 104: correlational analysis. *Singapore Medical Journal* 55:614-619.
323 Cunningham CB, Schilling N, Anders C, and Carrier DR. 2010. The influence of foot posture on the cost of
324   transport in humans. *Journal of Experimental Biology* 213:790-797. 10.1242/jeb.038984
325 Dagg AI. 1973. Gait in mammals. *Mammal Review* 3:135-154.
326 Fukuchi CA, Fukuchi RK, and Duarte M. 2019. Effects of walking speed on gait biomechanics in healthy
327   participants: a systematic review and meta-analysis. *Systematic Reviews* 8:153. 10.1186/s13643-
328   019-1063-z
329 Goslow Jr. GE, Reinking RM, and Stuart DG. 1973. The cat step cycle: Hind limb joint angles and muscle
330   lengths during unrestrained locomotion. 141:1-41. https://doi.org/10.1002/jmor.1051410102
331 Gossman MR, Rose SJ, Sahrmann SA, and Katholi CR. 1986. Length and circumference measurements in
332   one-joint and multijoint muscles in rabbits after immobilization. *Phys Ther* 66:516-520.
333   10.1093/ptj/66.4.516
334 Gushue DL, Houck J, and Lerner AL. 2005. Rabbit knee joint biomechanics: motion analysis and modeling
335   of forces during hopping. *J Orthop Res* 23:735-742. 10.1016/j.orthres.2005.01.005
336 Hall PT, Bratcher SZ, Stubbs C, Rifkin RE, Grzeskowiak RM, Burton BJ, Greenacre CB, Stephenson SM,
337   Anderson DE, and Crouch DL. 2021. Fully Implanted Prostheses for Musculoskeletal Limb
338   Reconstruction After Amputation: An In Vivo Feasibility Study. *Annals of Biomedical Engineering*
339   49:1012-1021. 10.1007/s10439-020-02645-3
340 Jarrell JR, Farrell BJ, Kistenberg RS, Dalton IV JF, Pitkin M, and Prilutsky BI. 2018. Kinetics of individual
341   limbs during level and slope walking with a unilateral transtibial bone-anchored prosthesis in the
342   cat. *Journal of Biomechanics* 76:74-83.
343 Kimura T. 1996. Correlation between the morphology of the feet and muscle fiber composition in the
344   anterior tibial muscle. *Anthropological Science* 104:1-14.
345 Koh TJ, and Herzog W. 1998a. Excursion is important in regulating sarcomere number in the growing
346   rabbit tibialis anterior. *The Journal of Physiology* 508:267-280.
347 Koh TJ, and Herzog W. 1998b. Increasing the moment arm of the tibialis anterior induces structural and
348   functional adaptation: implications for tendon transfer. *J Biomech* 31:593-599. 10.1016/s0021-
349   9290(98)00052-9
350 Lelas JL, Merriman GJ, Riley PO, and Kerrigan DC. 2003. Predicting peak kinematic and kinetic
351   parameters from gait speed. *Gait & Posture* 17:106-112. 10.1016/s0966-6362(02)00060-7
352 Li Y, and Hsiao-Wecksler E. 2013. Gait mode recognition and control for a portable-powered ankle-foot
353   orthosis. IEEE International Conference on Rehabilitation Robotics. p 1-8.
354 Liu C, Wang G, Zhou H, Mei Y, and Asafo-Duho BMK. 2020. Adaptability of Kinetic Parameters to a
355   Narrow Speed Range in Healthy Free-Moving Cats. *Mathematical Problems in Engineering*
356   2020:2954329. 10.1155/2020/2954329
357 Marghitu DB, Swaim SF, Rumph PF, Cojocaru D, Gillette RL, and Scardino MS. 2003. Dynamics Analysis of
358   Ground Contact Pressure of English Pointer Dogs. *Nonlinear Dynamics* 33:253-265.
359   10.1023/A:1026096111497

360 Mathis A, Mamidanna P, Abe T, Cury KM, Murthy VN, Mathis MW, and Bethge M. 2018a. Markerless
361   tracking of user-defined features with deep learning. *arXiv*. 10.48550/arXiv.1804.03142
362 Mathis A, Mamidanna P, Cury KM, Abe T, Murthy VN, Mathis MW, and Bethge M. 2018b. DeepLabCut:
363   markerless pose estimation of user-defined body parts with deep learning. *Nature Neuroscience*
364   21:1281-1289.
365 Mirkiani S, Roszko DA, O'Sullivan CL, Faridi P, Hu DS, Fang D, Everaert DG, Toossi A, Konrad PE, Robinson
366   K, and Mushahwar VK. 2022. Overground gait kinematics and muscle activation patterns in the
367   Yucatan mini pig. *Journal of Neural Engineering* 19. 10.1088/1741-2552/ac55ac
368 Nagasawa K, Noguchi M, Ikoma K, and Kubo T. 2008. Static and dynamic biomechanical properties of the
369   regenerating rabbit Achilles tendon. *Clinical Biomechhanics (Bristol, Avon)* 23:832-838.
370   10.1016/j.clinbiomech.2008.02.002
371 Oosterlinck M, Pille F, Huppes T, Gasthuys F, and Back W. 2010. Comparison of pressure plate and force
372   plate gait kinetics in sound Warmbloods at walk and trot. *The Veterinary Journal* 186:347-351.
373   https://doi.org/10.1016/j.tvjl.2009.08.024
374 Ponten E, and Friden J. 2008. Immobilization of the rabbit tibialis anterior muscle in a lengthened
375   position causes addition of sarcomeres in series and extra-cellular matrix proliferation. *Journal*
376   *of Biomechanics* 41:1801-1804. 10.1016/j.jbiomech.2008.03.006
377 Reddy GK, Stehno-Bittel L, and Enwemeka CS. 1998. Laser photostimulation of collagen production in
378   healing rabbit Achilles tendons. *Lasers in Surgery and Medicine* 22:281-287. 10.1002/(sici)1096-
379   9101(1998)22:5<281::aid-lsm4>3.0.co;2-l
380 Reddy NP, and Gupta V. 2007. Toward direct biocontrol using surface EMG signals: control of finger and
381   wrist joint models. *Medical Engineering & Physics* 29:398-403.
382   10.1016/j.medengphy.2005.10.016
383 Sheldon JD, Adkesson MJ, Allender MC, Bailey RS, Langan JN, and Chinnadurai SK. 2019. Evaluation of a
384   pressure sensitive walkway for objective gait analysis in normal and arthritic domestic ducks
385   (Cairina moschata domestica). *PLoS One* 14:e0220468.
386 Sjostrom M, Wahlby L, and Fugl-Meyer A. 1979. Achilles tendon injury. 3. Structure of rabbit soleus
387   muscles after immobilization at different positions. *Acta Chir Scand* 145:509-521.
388 Steiner R, Dhar M, Stephenson SM, Newby S, Bow A, Pedersen A, and Anderson DE. 2019. Biometric
389   Data Comparison Between Lewis and Sprague Dawley Rats. *Frontiers in Veterinary Science* 6.
390   10.3389/fvets.2019.00469
391 Tinga S, Kim SE, Banks SA, Jones SC, Park BH, Pozzi A, and Lewis DD. 2018. Femorotibial kinematics in
392   dogs with cranial cruciate ligament insufficiency: a three-dimensional in-vivo fluoroscopic
393   analysis during walking. *BMC Veterinary Research* 14:1-9.
394 Varejao AS, Cabrita AM, Meek MF, Bulas-Cruz J, Gabriel RC, Filipe VM, Melo-Pinto P, and Winter DA.
395   2002. Motion of the foot and ankle during the stance phase in rats. *Muscle & Nerve* 26:630-635.
396   10.1002/mus.10242
397 Verdugo MR, Rahal SC, Agostinho FS, Govoni VM, Mamprim MJ, and Monteiro FOB. 2013. Kinetic and
398   temporospatial parameters in male and female cats walking over a pressure sensing walkway.
399   *BMC Veterinary Research* 9:129. 10.1186/1746-6148-9-129
400 Vereecke E, D'Août K, De Clercq D, Van Elsacker L, and Aerts P. 2003. Dynamic plantar pressure
401   distribution during terrestrial locomotion of bonobos (Pan paniscus). *American Journal of*
402   *Physical Anthropology* 120:373-383. https://doi.org/10.1002/ajpa.10163
403 Vilensky JA. 1987. Locomotor behavior and control in human and non-human primates: comparisons
404   with cats and dogs. *Neurosci Biobehav Rev* 11:263-274. 10.1016/s0149-7634(87)80013-1
405 Volait-Rosset L, Pignon C, Manou M, and Donnelly TM. 2019. Surgical management of a calcaneus
406   fracture in a pet rabbit. *Journal of Exotic Pet Medicine* 29:110-114.

407

Figure 1

Testing setup used to collect biomechanical data.

(1) Tekscan Very HR Walkway 4 for measuring pressure data. **(2)** Acrylic tunnel for guiding rabbits across pressure mat. **(3)** 60 Hz Camera for recording sagittal plane kinematics.
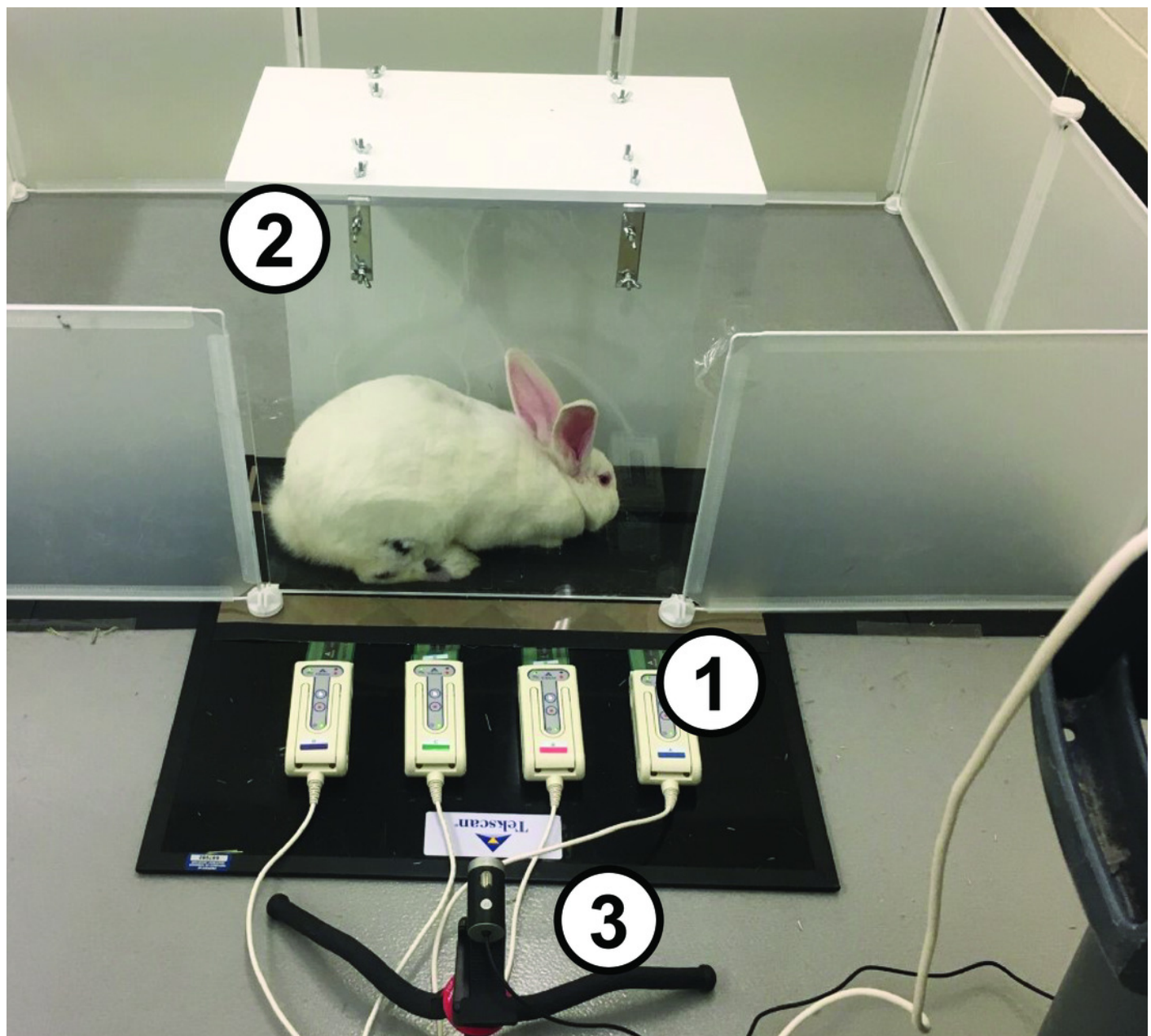
Figure 2

Motion capture analysis from sagittal plane videos for calculating hindlimb kinematics.

(A) Ink markers were placed on the lateral aspect of the hindlimb approximately over the knee, ankle, and metatarsophalangeal (MTP) joint centers. **(B)** A frame-by-frame bottom-hat morphology permitted detection of joint markers. **(C)** Vectors representing limb segments (orange lines) were drawn between the centroids of the joint markers. Using the dot product and the segment vectors, we calculated the ankle angle (yellow) and foot angle (blue).
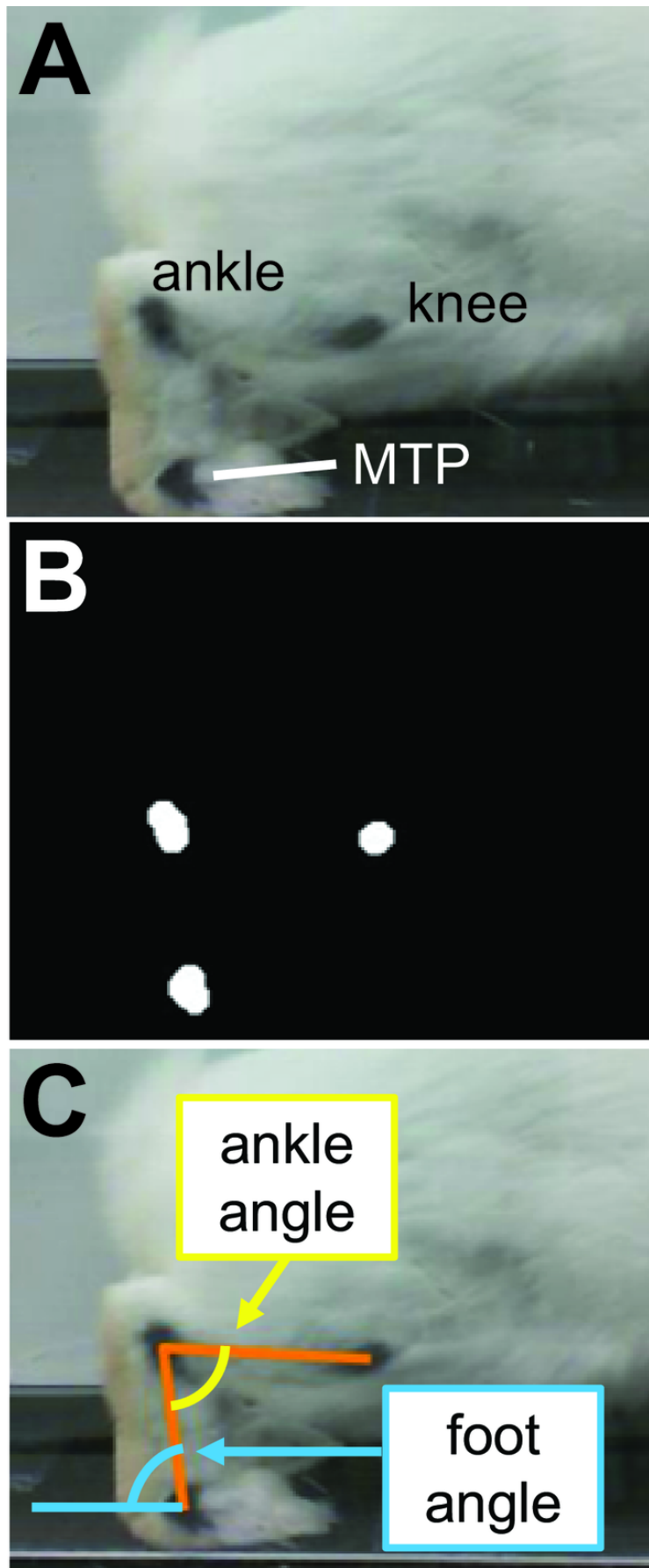
Figure 3

Joint kinematics of the rabbit hindlimb during stance phase.

Mean (black line) and ±1 standard deviation (grey shaded region) of **(A)** ankle angle and **(B)** foot angle. Consistent with previous descriptions of gait (Li & Hsiao-Wecksler 2013), we divided rabbit stance into "loading response" and "propulsion" sub-phases at the maximum ankle dorsiflexion (i.e., smallest value) angle (grey dotted line).
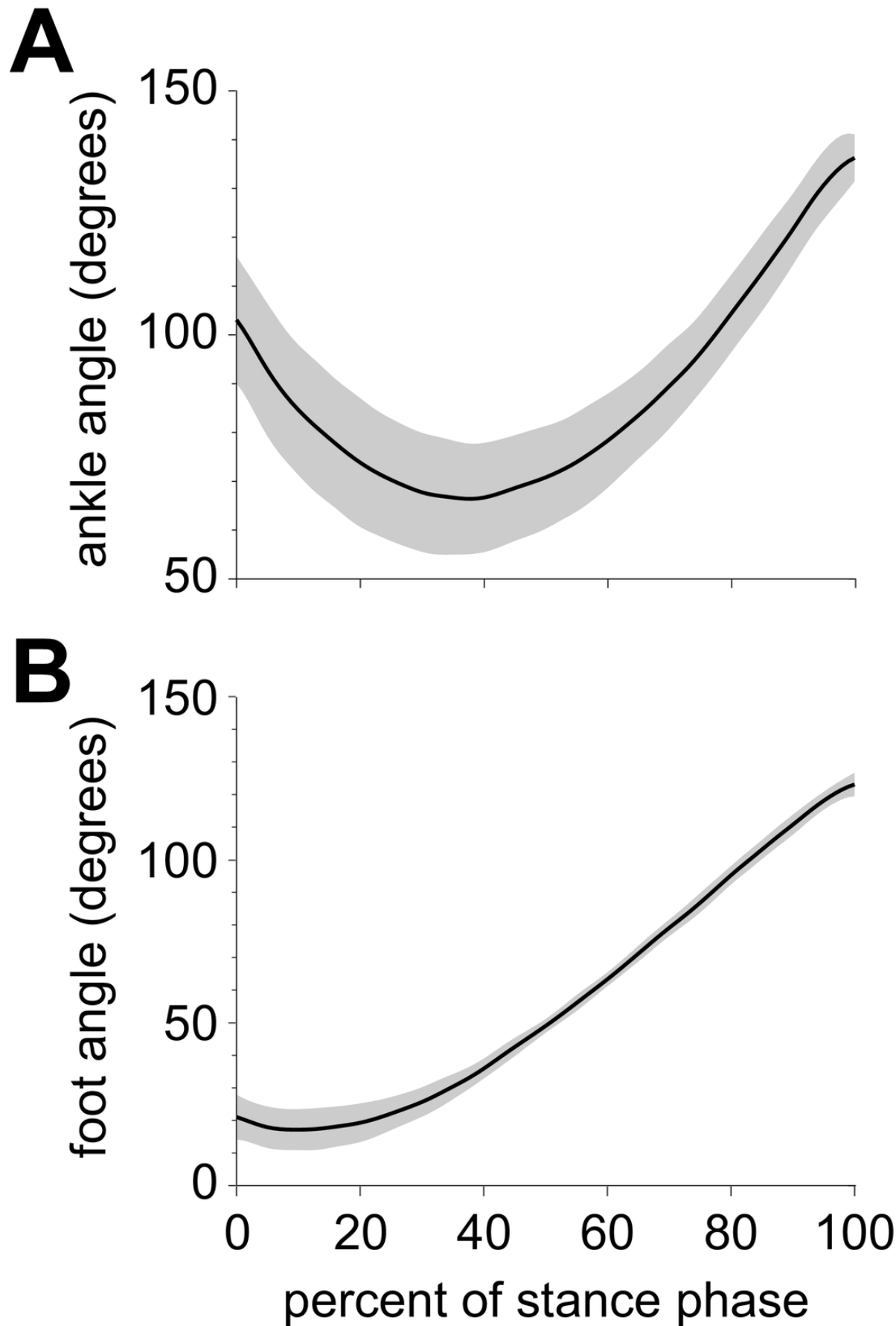
Figure 4

Plantar pressures of the rabbit hindlimb during stance phase.

Mean (black line) and ±1 standard deviation (grey shaded region) of **(B)** peak plantar pressure and **(C)** average plantar pressure. Both pressures were normalized by body weight.
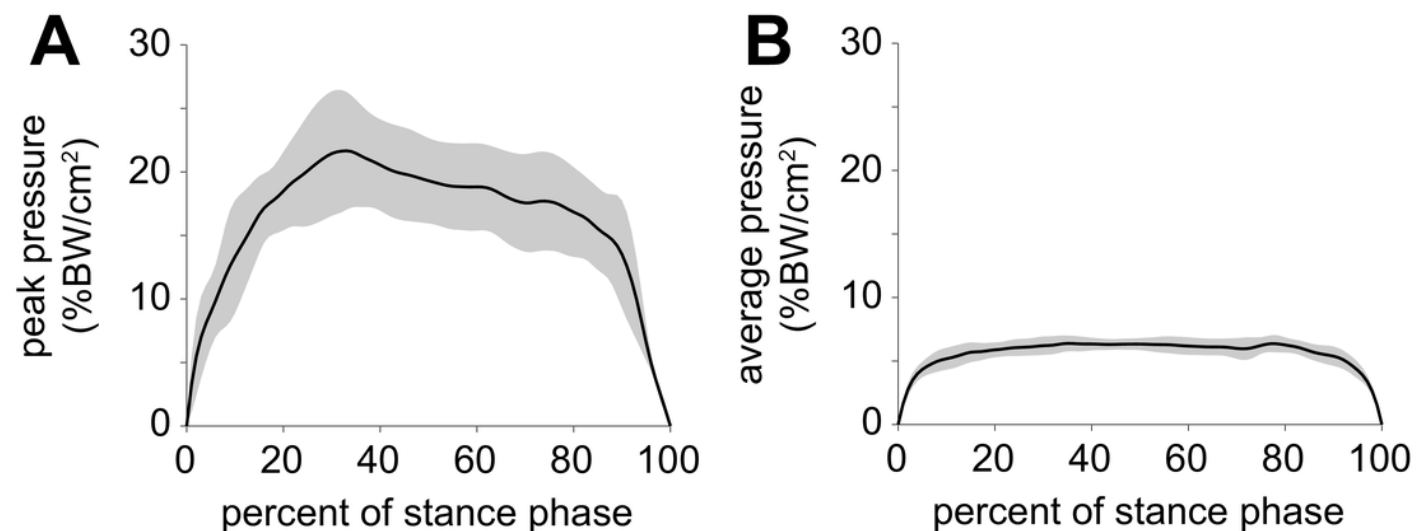
Figure 5

Net vertical ground reaction force (vGRF) of the rabbit hindlimb during stance phase.

vGRF was expressed as a percentage of body weight (%BW). Black line and grey shaded region indicate the mean and ±1 standard deviation, respectively.
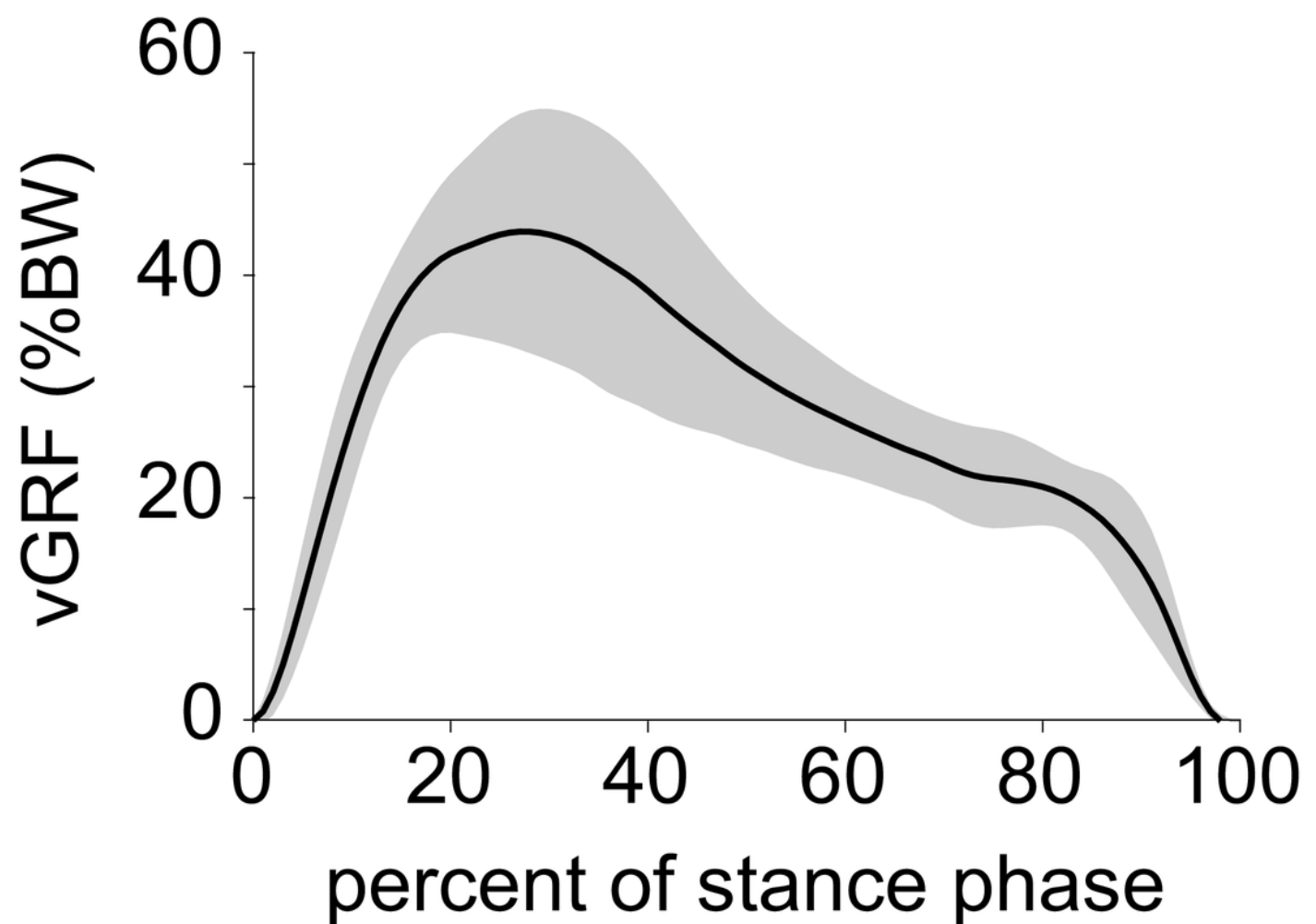
Figure 6

Plantar contact area of the rabbit hindlimb during stance phase.

Black line and grey shaded region indicate the mean and ±1 standard deviation, respectively.
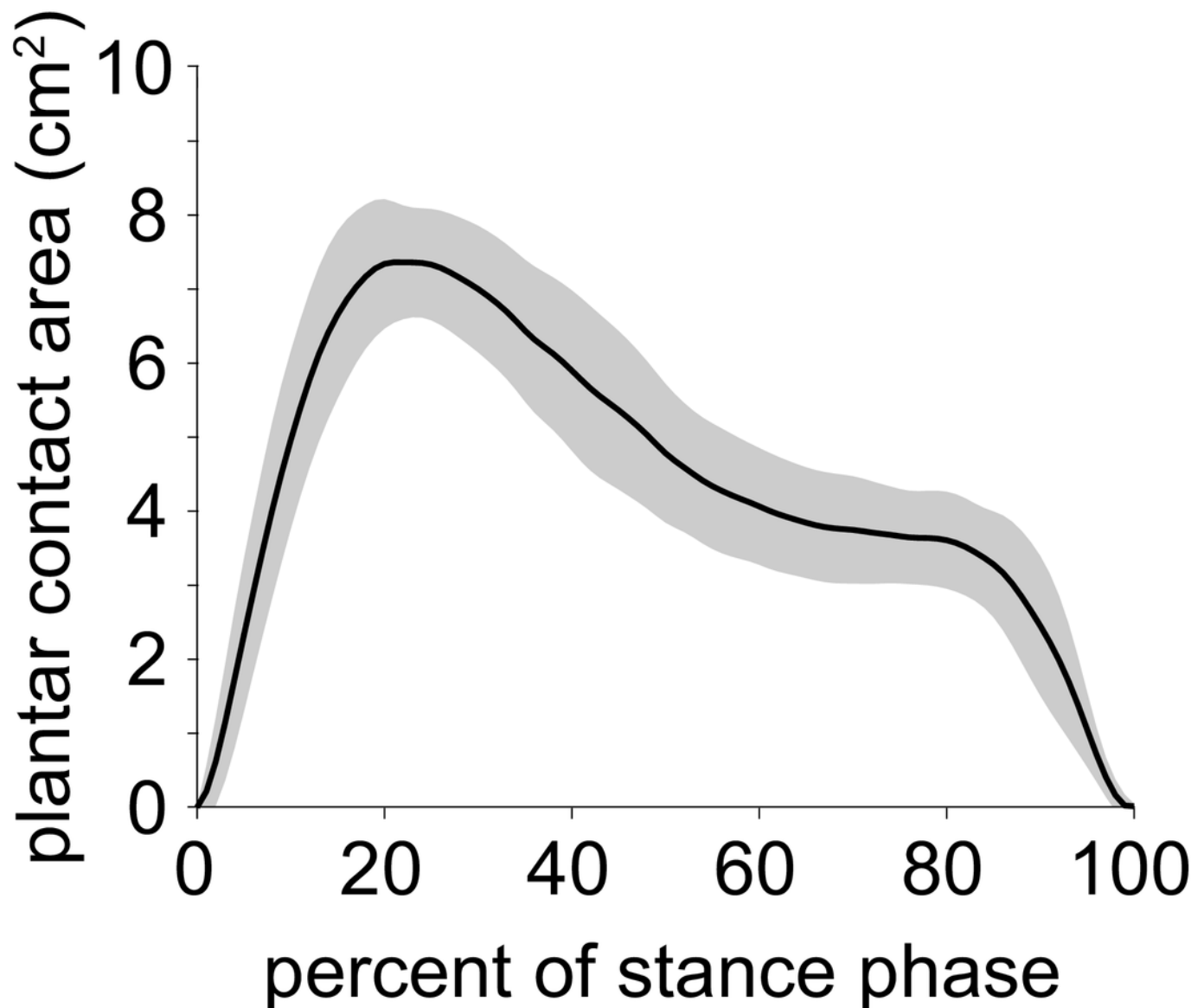
Select biomechanical variables and their correlation with stance duration.

Spearman's rank-order correlation test was performed to compute the correlation coefficient, rho (ρ). P-values were computed to determine the statistical significance of the correlation.

biomechanical variable	mean ± SD (n=6 rabbits)	correlation with stance duration (n=49 trials)	
		Spearman's rho (ρ)	p
stance duration (s)	0.40 ± 0.15	---	---
maximum foot angle (deg)	123.3 ± 3.6	0.41	0.003
minimum foot angle (deg)	17.2 ± 6.3	-0.58	<0.001
maximum ankle angle (deg)	137.2 ± 4.8	-0.13	0.363
minimum ankle angle (deg)	66.4 ± 13.4	-0.30	0.034
maximum plantar contact area (cm^2)	7.4 ± 0.8	0.03	0.815
plantar contact length (%)	70 ± 11	0.52	<0.001
maximum peak plantar pressure (%BW/cm^2)	0.217 ± 0.046	-0.24	0.092
maximum vGRF (%BW)	44.0 ± 10.6	-0.35	0.014
vertical impulse (%BW·s)	10.9 ± 3.7	0.76	<0.001